A Unified Concept for Controlling a Marine Surface Vessel Through the Entire Speed Envelope

Morten Breivik*,[1]
*Centre for Ships and Ocean Structures (CESOS)
Norwegian University of Science and Technology (NTNU)
NO-7491 Trondheim, Norway
E-mail: morten.breivik@ieee.org

Thor I. Fossen*,†
†Department of Engineering Cybernetics (ITK)
Norwegian University of Science and Technology (NTNU)
NO-7491 Trondheim, Norway
E-mail: fossen@ieee.org

***Abstract*— This paper addresses the problem of creating a controller structure for the automatic control of a marine surface vessel through its entire speed regime without resorting to heuristics and switching between fundamentally different controllers. Hence, a single controller structure is proposed for the purpose. Its core is a nonlinear, model-based velocity and heading controller which relies on a key guidance-based path following concept necessary to ensure geometric path convergence. The scheme renders all regular paths feasible, and ensures that a vessel which is fully actuated at low speeds, but becomes underactuated at high speeds, is able to converge to and follow a desired geometric path independent of the current vessel speed.**

I. Introduction

It is a fundamental necessity to be able to automatically control a marine surface vessel through its entire speed regime, i.e. through all the stages from low-speed positioning to high-speed maneuvers. Traditionally, such a problem has been solved by constructing dedicated controllers for each distinct part of the speed envelope. The desired functionality is then achieved by designing a high-level decision-making system to intelligently switch between the different controllers, resulting in a hybrid and discontinous system. Usually, a nonlinear, model-based controller is designed for low-speed applications, and it is assumed that the vessel in question is fully actuated for the purpose, i.e. independently actuated in all degrees-of-freedom (DOFs) simultaneously. For high-speed applications, a linear heading controller based on the Nomoto model is usually designed, together with an independent speed controller. At high speeds, the vessel is for all practical purposes underactuated, i.e. it lacks the capability to command independent accelerations in all DOFs simultaneously.

Being able to design a single controller structure, i.e. without heuristics and hybrid switching, to cover the entire speed envelope of a marine surface vessel, would be very desirable from both a theoretical and industrial point of view. Theoretically, for obvious reasons such as stability results. Industrially, for reasons such as reduced complexity of implementation, easier code verification and maintenance procedures, and possibly increased safety of operation.

In practice, the only relevant type of vessels to consider are the ones which become underactuated in the sway direction (lateral direction) at high speeds. These are typically equipped with a number of tunnel thrusters both fore and aft, designed to assist at low-speed maneuvers, which are rendered inoperable at high speeds mainly due to the relative water speed past their outlets. Under such circumstances the only means of actuation are the main propulsors located aft. An example of such a vessel is a tugboat from Rolls-Royce Marine, which is illustrated in Figure 1.

A. Previous Work

An interesting paper which treats the desired control topic is [1], where a hybrid switching design between a dynamic positioning controller for low speeds and a track-keeping controller for high speeds is considered for minehunters in the Italian Navy. A similar hybrid procedure is presented in [2], where the application is high-speed craft powered mainly by waterjets. Hybrid designs for offshore supply vessels are mentioned in [3]. However, compared to traditional industrial control schemes where the helmsman is required to exert manual control during part of the speed envelope, the designs presented in these papers represent a step forward.

B. Main Contribution

This paper presents a single controller structure capable of controlling a marine surface vessel through its entire speed envelope. The core of the structure consists of a nonlinear, model-based velocity and heading controller which relies on a key guidance-based path following concept necessary to guarantee geometric path convergence. The scheme is a natural extension of the path following approach in [4] where the individual designs for the fully actuated and the underactuated vessels have been fusioned into one, seamless, continous design without any heuristics involved. The paper contains a lucid exposition of the proposed approach, which has an intuitive physical interpretation.

[1]This work was supported by the Research Council of Norway through the Centre for Ships and Ocean Structures at NTNU.

II. Problem Statement

The primary objective in guidance-based path following is to ensure that a vehicle converges to and follows a desired geometric path, without any temporal requirements. The secondary objective is to ensure that the vehicle complies with a desired dynamic behaviour. By using the convenient task classification scheme of [5], the guidance-based path following problem can thus be expressed by the following two task objectives:

Geometric Task: Make the position of the vehicle converge to and follow a desired geometric path.

Dynamic Task: Make the speed of the vehicle converge to and track a desired speed assignment.

III. Guidance System Design

This section develops the guidance laws required to solve the planar guidance-based path following problem in question. Throughout the section we will consistently employ the notion of an *ideal particle*, which is to be interpreted as a planar position variable without dynamics, i.e. it can instantly attain any assigned motion behaviour. The developed guidance laws can subsequently be extended to any desirable dynamics case since they are generically valid.

A. Assumptions

The following assumptions are made:

- **A.1** The desired geometric path is regularly parametrized.
- **A.2** The speed of the ideal particle is lower-bounded, i.e. $U_d(t) \in [U_{d,\min}, \infty\rangle \ \forall t \geq 0$.
- **A.3** The guidance variable is positive and upper-bounded, i.e. $\triangle(t) \in \langle 0, \triangle_{\max}] \ \forall t \geq 0$.

B. Guidance Law Design

Denote the inertial position and velocity vectors of the ideal particle by $\mathbf{p} = [x, y]^\top \in \mathbb{R}^2$ and $\mathbf{v} = \dot{\mathbf{p}} = [\dot{x}, \dot{y}]^\top \in \mathbb{R}^2$, respectively. Denote the size of the velocity vector by $U = |\mathbf{v}|_2 = (\mathbf{v}^\top \mathbf{v})^{\frac{1}{2}}$ (the speed) and its orientation by $\chi = \arctan(\frac{\dot{y}}{\dot{x}})$ (the azimuth angle). Since it is assumed that both U and χ can attain any desirable value instantaneously, they are rewritten as U_d and χ_d. Then consider a geometric path continuosly parametrized by a scalar variable $\theta \in \mathbb{R}$, and denote the inertial position of a point belonging to the path as $\mathbf{p}_d(\theta) \in \mathbb{R}^2$. The desired geometric path can consequently be expressed by the set:

$$\mathcal{P} = \left\{ \mathbf{p} \in \mathbb{R}^2 \mid \mathbf{p} = \mathbf{p}_d(\theta) \ \forall \theta \in \mathbb{R} \right\}, \tag{1}$$

where $\mathcal{P} \subset \mathbb{R}^2$. For a given θ, define a local reference frame at $\mathbf{p}_d(\theta)$ and name it the Path Parallel (PP) frame. The PP frame is rotated an angle:

$$\chi_t(\theta) = \arctan\left(\frac{y_d'(\theta)}{x_d'(\theta)} \right) \tag{2}$$

relative to the inertial frame, where the notation $x_d'(\theta) = \frac{dx_d}{d\theta}(\theta)$ has been utilized. Consequently, the x-axis of the PP frame is aligned with the tangent vector to the path at $\mathbf{p}_d(\theta)$, see Figure 2. The error vector between $\mathbf{p}$ and $\mathbf{p}_d(\theta)$ expressed in the PP frame is given by:

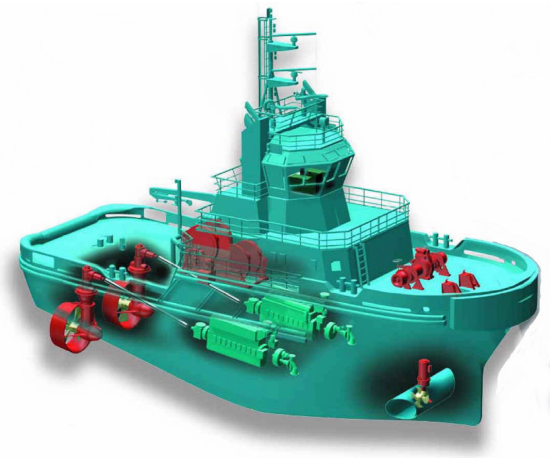

Fig. 1. A principle drawing of a tugboat with two main azimuth thrusters aft and one tunnel thruster in the bow. Courtesy of Rolls-Royce Marine, http://www.rolls-royce.com/marine/.

$$\boldsymbol{\varepsilon} = \mathbf{R}_t^\top (\mathbf{p} - \mathbf{p}_d(\theta)), \tag{3}$$

where:

$$\mathbf{R}_t(\chi_t) = \begin{bmatrix} \cos\chi_t & -\sin\chi_t \\ \sin\chi_t & \cos\chi_t \end{bmatrix} \tag{4}$$

is the rotation matrix from the inertial frame to the PP frame, $\mathbf{R}_t \in SO(2)$. The error vector $\boldsymbol{\varepsilon} = [s, e]^\top \in \mathbb{R}^2$ consists of the *along-track error* s and the *cross-track error* e, see Figure 2. Also, recognize the concept of the *off-track error*, represented by $|\boldsymbol{\varepsilon}|_2 = \sqrt{\boldsymbol{\varepsilon}^\top \boldsymbol{\varepsilon}} = \sqrt{s^2 + e^2}$.

Define the positive definite and radially unbounded Control Lyapunov Function (CLF):

$$V_{\boldsymbol{\varepsilon}} = \frac{1}{2} \boldsymbol{\varepsilon}^\top \boldsymbol{\varepsilon} = \frac{1}{2}(s^2 + e^2), \tag{5}$$

and differentiate it with respect to time along the trajectories of $\boldsymbol{\varepsilon}$ to obtain:

$$\dot{V}_{\boldsymbol{\varepsilon}} = s(U_d \cos(\chi_d - \chi_t) - U_{PP}) + eU_d \sin(\chi_d - \chi_t). \tag{6}$$

We can clearly consider the path tangential speed U_{PP} as a virtual input for stabilizing s, so by choosing:

$$U_{PP} = U_d \cos(\chi_d - \chi_t) + \gamma s, \tag{7}$$

where $\gamma > 0$ becomes a constant gain parameter in the guidance law, we achieve:

$$\dot{V}_{\boldsymbol{\varepsilon}} = -\gamma s^2 + eU_d \sin(\chi_d - \chi_t). \tag{8}$$

From (8) we see that $(\chi_d - \chi_t)$ can be considered a virtual input for stabilizing e. Denote this angular difference by $\chi_r = \chi_d - \chi_t$, i.e. the relative angle between the desired azimuth angle and the azimuth angle of the path tangential. Obviously, such a variable should depend on the cross-track

error itself, such that $\chi_r = \chi_r(e)$. An attractive choice for $\chi_r(e)$ could be the physically motivated:

$$\chi_r(e) = \arctan\left(-\frac{e}{\triangle}\right), \tag{9}$$

where $\triangle > 0$ becomes a time-varying guidance variable utilized to shape the convergence behaviour towards the path tangential, i.e. $\triangle = \triangle(t)$ satisfying A.3. It is often referred to as the *lookahead distance* in literature dealing with path following along straight lines [6], and the physical interpretation can be derived from Figure 2. Other sigmoidal shaping functions are also possible candidates for $\chi_r(e)$. The desired azimuth angle is thus given by:

$$\chi_d(\theta, e) = \chi_t(\theta) + \chi_r(e) \tag{10}$$

with $\chi_t(\theta)$ as in (2) and $\chi_r(e)$ as in (9). We also need to state the relationship between θ and U_{PP}:

$$\begin{aligned} \dot{\theta} &= \frac{U_{PP}}{\sqrt{x_d'^2 + y_d'^2}} \\ &= \frac{U_d \cos\chi_r + \gamma s}{\sqrt{x_d'^2 + y_d'^2}}, \end{aligned} \tag{11}$$

which is non-singular for all paths satisfying assumption A.1. Hence, the derivative of the CLF finally becomes:

$$\begin{aligned} \dot{V}_{\boldsymbol{\varepsilon}} &= -\gamma s^2 + e U_d \sin\chi_r \\ &= -\gamma s^2 - U_d \frac{e^2}{\sqrt{e^2 + \triangle^2}}, \end{aligned} \tag{12}$$

which is negative definite under assumptions A.2 and A.3. The last transition is made by utilizing trigonometric relationships from Figure 2. Note that the speed by definition cannot be negative.

Elaborating on these results, we find that the error system can be represented by the states $\boldsymbol{\varepsilon}$ and θ. It can be rendered autonomous by reformulating its time dependence through the introduction of an extra state:

$$\dot{l} = 1, \; l_0 = t_0 \geq 0, \tag{13}$$

see e.g. [7]. The new and extended system can be represented by the state vector $\mathbf{x} = \left[\boldsymbol{\varepsilon}^\top, \theta, l\right]^\top \in \mathbb{R}^2 \times \mathbb{R} \times \mathbb{R}_{\geq 0}$, with the dynamics:

$$\dot{\mathbf{x}} = \mathbf{f}(\mathbf{x}). \tag{14}$$

The time variable for this new system is denoted t with initial time $t = 0$, such that $l(t) = t + t_0$. We can now utilize set-stability analysis for time-invariant systems in order to be able to conclude on the task objectives in the problem statement. Hence, define the closed, but non-compact set:

$$\mathcal{G} = \left\{\mathbf{x} \in \mathbb{R}^2 \times \mathbb{R} \times \mathbb{R}_{\geq 0} \mid \boldsymbol{\varepsilon} = \mathbf{0}\right\}, \tag{15}$$

which represents the dynamics of the extended system when the ideal particle has converged to the path. Also, let:

$$\begin{aligned} |\mathbf{x}|_{\mathcal{G}} &= \inf\left\{\mathbf{x} - \mathbf{y} \mid \mathbf{y} \in \mathcal{G}\right\} && (16) \\ &= |(\boldsymbol{\varepsilon}, 0, 0)|_2 && (17) \\ &= (\boldsymbol{\varepsilon}^\top \boldsymbol{\varepsilon})^{\frac{1}{2}} && (18) \end{aligned}$$

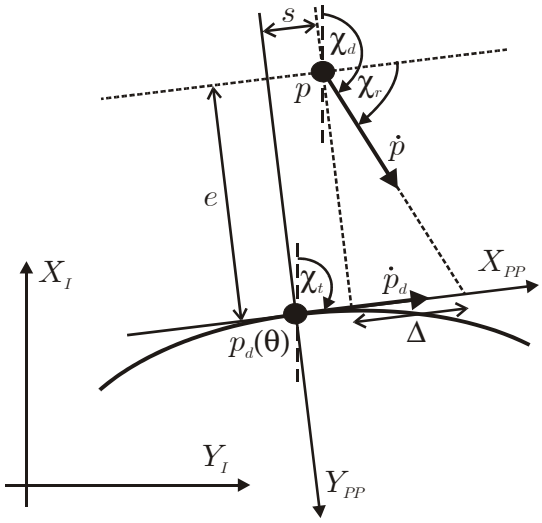

Fig. 2. The geometric relationships between the relevant parameters and variables utilized in the guidance-based path following scheme.

represent a function measuring the distance from $\mathbf{x}$ to the set $\mathcal{G}$, i.e. the previously mentioned off-track error. The goal is consequently to make $|\mathbf{x}|_{\mathcal{G}}$ converge to zero since it is equivalent to solving the geometric task of the guidance-based path following problem. The following proposition can now be stated:

Proposition 1: The error set $\mathcal{G}$ is rendered uniformly globally asymptotically and locally exponentially stable (UGAS/ULES) under assumptions A.1-A.3 if χ_r is equal to (9) and θ is updated by (11).

Proof: [Indication] By establishing that (14) is forward complete and $\mathcal{G}$ is forward invariant, we can derive our stability results by simply considering $V_{\boldsymbol{\varepsilon}} = \frac{1}{2}\boldsymbol{\varepsilon}^\top\boldsymbol{\varepsilon} = \frac{1}{2}|\mathbf{x}|^2_{\mathcal{G}}$, see e.g. [5]. Hence, by standard Lyapunov arguments the error set $\mathcal{G}$ is rendered UGAS under assumptions A.1-A.3 when (9) and (11) are satisfied. Furthermore, $\dot{V}_{\boldsymbol{\varepsilon}} \leq -\gamma s^2 - \frac{U_{d,\min}}{\triangle_{\max}} e^2$ for the error dynamics at $\boldsymbol{\varepsilon} = \mathbf{0}$, which proves ULES. ■

By choosing the speed of the ideal particle equal to:

$$U_d = \kappa\sqrt{e^2 + \triangle^2}, \tag{19}$$

where $\kappa > 0$ is a constant gain parameter, we obtain:

$$\dot{V}_{\boldsymbol{\varepsilon}} = -\gamma s^2 - \kappa e^2, \tag{20}$$

which results in the following proposition:

Proposition 2: The error set $\mathcal{G}$ is rendered uniformly globally exponentially stable (UGES) under assumptions A.1 and A.3 if χ_r is equal to (9), θ given by (11) and U_d satisfies (19).

Proof: [Indication] The first part of the proof is identical to that of Proposition 1. Hence, we conclude by standard Lyapunov arguments that the error set $\mathcal{G}$ is rendered UGES. ■

Although very powerful, this result is clearly not achievable by physical systems since these exhibit natural limitations on their maximum attainable speed. In this regard, Proposition 1 states the best possible stability property a planar physical system like a marine surface vessel can hold.

IV. Control System Design

The 3 DOF kinematics and kinetics of a marine surface vessel can be represented by [8]:

$$\dot{\boldsymbol{\eta}} = \mathbf{R}(\psi)\boldsymbol{\nu} \tag{21}$$

and:

$$\mathbf{M}\dot{\boldsymbol{\nu}} + \mathbf{C}(\boldsymbol{\nu})\boldsymbol{\nu} + \mathbf{D}(\boldsymbol{\nu})\boldsymbol{\nu} = \boldsymbol{\tau} + \mathbf{R}(\psi)^\top \mathbf{b}, \tag{22}$$

where $\boldsymbol{\eta} = [x, y, \psi]^\top \in \mathbb{R}^3$ represents the earth-fixed position and heading, $\boldsymbol{\nu} = [u, v, r]^\top \in \mathbb{R}^3$ represents the vessel-fixed velocities, $\mathbf{R}(\psi) \in SO(3)$ is the rotation matrix from the earth-fixed local geographic reference frame (NED) to the vessel-fixed reference frame (BODY), $\mathbf{M}$ is the vessel inertia matrix, $\mathbf{C}(\boldsymbol{\nu})$ is the centrifugal and coriolis matrix, and $\mathbf{D}(\boldsymbol{\nu})$ is the hydrodynamic damping matrix. The system matrices in (22) are assumed to satisfy the properties $\mathbf{M} = \mathbf{M}^\top > 0$, $\mathbf{C} = -\mathbf{C}^\top$ and $\mathbf{D} > 0$. Furthermore, $\boldsymbol{\tau}$ represents the vessel-fixed propulsion forces and moments, and $\mathbf{b}$ describes the low frequency environmental forces acting on the vessel.

A. Control Law Design

A nonlinear, model-based velocity and heading controller is designed by using the backstepping technique. The output-to-be-controlled has been redefined from position and heading to velocity and heading, so by feeding the controller with the appropriate reference signals, positional convergence is ensured such that the path following task objectives are satisfied. This approach resembles the real-life action of a helmsman onboard a vessel more closely than direct position control in the sense that he uses the vessel velocity to maneuver. He does not think in terms of controlling the position directly, but in his mind feeds the position error signal back through the velocity assignment, ensuring position control indirectly through direct velocity control. Such a technique is equally favourable for fully actuated and underactuated vessels, hence the chosen controller assumes the form of a velocity and heading controller.

Start by defining the projection vector $\mathbf{h}$:

$$\mathbf{h} = [0, 0, 1]^\top, \tag{23}$$

then the error variables $z_1 \in \mathbb{R}$ and $\mathbf{z}_2 \in \mathbb{R}^3$ according to:

$$\begin{aligned} z_1 &= \psi - \psi_d = \mathbf{h}^\top \boldsymbol{\eta} - \psi_d & (24)\\ \mathbf{z}_2 &= [z_{2,1}, z_{2,2}, z_{2,3}]^\top = \boldsymbol{\nu} - \boldsymbol{\alpha}, & (25) \end{aligned}$$

where $\boldsymbol{\alpha} = [\alpha_1, \alpha_2, \alpha_3]^\top \in \mathbb{R}^3$ is a vector of stabilizing functions to be specified later.

Step 1:

Define the first Control Lyapunov Function (CLF) as:

$$V_1 = \frac{1}{2} k_1 z_1^2, \tag{26}$$

where $k_1 > 0$. Differentiating V_1 with respect to time along the z_1-dynamics yields:

$$\begin{aligned} \dot{V}_1 &= k_1 z_1 \dot{z}_1 \\ &= k_1 z_1 (\mathbf{h}^\top \dot{\boldsymbol{\eta}} - \dot{\psi}_d) \\ &= k_1 z_1 (\mathbf{h}^\top \boldsymbol{\nu} - \dot{\psi}_d), \end{aligned} \tag{27}$$

since $\dot{\boldsymbol{\eta}} = \mathbf{R}\boldsymbol{\nu}$ and $\mathbf{h}^T \mathbf{R} \boldsymbol{\nu} = \mathbf{h}^T \boldsymbol{\nu}$. By using (25), we obtain:

$$\begin{aligned} \dot{V}_1 &= k_1 z_1 (\mathbf{h}^\top (\mathbf{z}_2 + \boldsymbol{\alpha}) - \dot{\psi}_d) \\ &= k_1 z_1 \mathbf{h}^\top \mathbf{z}_2 + k_1 z_1 (\alpha_3 - \dot{\psi}_d). \end{aligned} \tag{28}$$

This motivates the choice of the stabilizing function α_3 as:

$$\alpha_3 = \dot{\psi}_d - z_1, \tag{29}$$

which results in:

$$\dot{V}_1 = -k_1 z_1^2 + k_1 z_1 \mathbf{h}^\top \mathbf{z}_2. \tag{30}$$

Step 2:

Augment the first CLF to obtain:

$$V_2 = V_1 + \frac{1}{2} \mathbf{z}_2^\top \mathbf{M} \mathbf{z}_2 + \frac{1}{2} \tilde{\mathbf{b}}^\top \boldsymbol{\Gamma}^{-1} \tilde{\mathbf{b}}, \tag{31}$$

where $\tilde{\mathbf{b}} \in \mathbb{R}^3$ is an adaptation error defined as $\tilde{\mathbf{b}} = \hat{\mathbf{b}} - \mathbf{b}$ with $\hat{\mathbf{b}}$ being the estimate of $\mathbf{b}$, and by assumption $\dot{\mathbf{b}} = \mathbf{0}$. $\boldsymbol{\Gamma} = \boldsymbol{\Gamma}^\top > 0$ is the adaptation gain matrix.

Differentiating V_2 along the trajectories of z_1, $\mathbf{z}_2$ and $\tilde{\mathbf{b}}$, we obtain:

$$\dot{V}_2 = -k_1 z_1^2 + k_1 z_1 \mathbf{h}^\top \mathbf{z}_2 + \mathbf{z}_2^\top \mathbf{M} \dot{\mathbf{z}}_2 + \tilde{\mathbf{b}}^\top \boldsymbol{\Gamma}^{-1} \dot{\tilde{\mathbf{b}}}, \tag{32}$$

since $\mathbf{M} = \mathbf{M}^\top$ and $\dot{\tilde{\mathbf{b}}} = \dot{\hat{\mathbf{b}}}$. The fact that:

$$\begin{aligned} \mathbf{M}\dot{\mathbf{z}}_2 &= \mathbf{M}(\dot{\boldsymbol{\nu}} - \dot{\boldsymbol{\alpha}}) \\ &= \boldsymbol{\tau} + \mathbf{R}^\top \mathbf{b} - \mathbf{C}(\boldsymbol{\nu})\boldsymbol{\nu} - \mathbf{D}(\boldsymbol{\nu})\boldsymbol{\nu} - \mathbf{M}\dot{\boldsymbol{\alpha}} \end{aligned} \tag{33}$$

yields:

$$\begin{aligned} \dot{V}_2 &= -k_1 z_1^2 + \mathbf{z}_2^\top (\mathbf{h} k_1 z_1 + \boldsymbol{\tau} + \mathbf{R}^\top \mathbf{b} - \mathbf{C}(\boldsymbol{\nu})\boldsymbol{\nu}) + \\ &\quad \mathbf{z}_2^\top (-\mathbf{D}(\boldsymbol{\nu})\boldsymbol{\nu} - \mathbf{M}\dot{\boldsymbol{\alpha}}) + \tilde{\mathbf{b}}^\top \boldsymbol{\Gamma}^{-1} \dot{\hat{\mathbf{b}}}. \end{aligned} \tag{34}$$

By rewriting $\mathbf{C}(\boldsymbol{\nu}) = \mathbf{C}$ and $\mathbf{D}(\boldsymbol{\nu}) = \mathbf{D}$ for notational brevity, and utilizing the fact that $\boldsymbol{\nu} = \mathbf{z}_2 + \boldsymbol{\alpha}$ and $\mathbf{b} = \hat{\mathbf{b}} - \tilde{\mathbf{b}}$, we obtain:

$$\begin{aligned} \dot{V}_2 &= -k_1 z_1^2 - \mathbf{z}_2^\top \mathbf{C}\mathbf{z}_2 - \mathbf{z}_2^\top \mathbf{D}\mathbf{z}_2 + \\ &\quad \mathbf{z}_2^\top (\mathbf{h} k_1 z_1 + \boldsymbol{\tau} + \mathbf{R}^\top \hat{\mathbf{b}} - \mathbf{C}\boldsymbol{\alpha} - \mathbf{D}\boldsymbol{\alpha} - \mathbf{M}\dot{\boldsymbol{\alpha}}) + \\ &\quad \tilde{\mathbf{b}}^\top \boldsymbol{\Gamma}^{-1} (\dot{\hat{\mathbf{b}}} - \boldsymbol{\Gamma}\mathbf{R}\mathbf{z}_2), \end{aligned} \tag{35}$$

where $\mathbf{z}_2^\top \mathbf{C}\mathbf{z}_2 = 0$ since $\mathbf{C}$ is skew-symmetric [8]. By assigning:

$$\boldsymbol{\tau} = \mathbf{M}\dot{\boldsymbol{\alpha}} + \mathbf{C}\boldsymbol{\alpha} + \mathbf{D}\boldsymbol{\alpha} - \mathbf{R}^\top \hat{\mathbf{b}} - \mathbf{h} k_1 z_1 - \mathbf{K}_2 \mathbf{z}_2, \tag{36}$$

where $\mathbf{K}_2 = diag(k_{2,1}, k_{2,2}, k_{2,3}) > 0$, and by choosing:

$$\dot{\hat{\mathbf{b}}} = \mathbf{\Gamma R z}_2, \tag{37}$$

we finally obtain:

$$\dot{V}_2 = -k_1 z_1^2 - \mathbf{z}_2^\top (\mathbf{D} + \mathbf{K}_2)\mathbf{z}_2. \tag{38}$$

We choose $\alpha_1 = u_d$, but currently postpone the choice of α_2. Choosing α_2 is vital to the desirable system behaviour, but since equation (36) is valid as long as α_2, $\dot{\alpha}_2 \in \mathcal{L}_\infty$, it is already possible to summarize the control law design by the following proposition:

Proposition 3: For smooth reference trajectories ψ_d, $\dot{\psi}_d$, $\ddot{\psi}_d \in \mathcal{L}_\infty$, u_d, $\dot{u}_d \in \mathcal{L}_\infty$ and α_2, $\dot{\alpha}_2 \in \mathcal{L}_\infty$, the origin of the error system $\left[z_1, \mathbf{z}_2^\top, \tilde{\mathbf{b}}^\top\right]^\top$ becomes UGAS/ULES by choosing the control and disturbance adaptation laws as in (36) and (37), respectively.

Proof: [Indication] The proof can be straightforwardly carried out by utilizing Theorem A.5 from [8]. ■

B. A Unified Control Law Concept

The control vector of a fully actuated vessel is given by:

$$\boldsymbol{\tau} = [\tau_1, \tau_2, \tau_3]^\top, \tag{39}$$

where τ_1 represents the force input in surge, τ_2 represents the force input in sway, and τ_3 represents the moment input in yaw. On the other hand, the control vector of a sway-underactuated vessel is given by:

$$\boldsymbol{\tau} = [\tau_1, 0, \tau_3]^\top. \tag{40}$$

Equation (36) is kept valid in the fully actuated case by assigning the required expressions to all of $\boldsymbol{\tau}$. In the underactuated case it can still be kept valid by assigning the required expressions to τ_1 and τ_3, while simultaneously imposing dynamics on the sway stabilizing function α_2 such that (36) is satisfied [9]. An analysis of the resulting α_2-subsystem reveals that the stabilizing function, and hence also the sway speed, remains bounded. This is an inherent feature of the ambient water-vessel system due to the desirable property of hydrodynamic damping.

Elaborating on the facts above, imagine a weighting variable $\sigma \in [0, 1]$ with the following properties:

- $\sigma = 1$ indicates a fully actuated vessel.
- $\sigma = 0$ indicates an underactuated vessel.

Such a variable could be implemented as a sigmoidal function, ensuring a smooth transition between a fully actuated and an underactuated vessel. A natural choice would be to make it dependent of the instantaneous vessel speed, i.e. $\sigma = \sigma(U)$. Now, consider a vessel with a transitional speed zone between full actuation and underactuation represented by a lower limit of U_f corresponding to a speed where it is still fully actuated, and an upper limit of U_u corresponding to a speed where it has become underactuated. Then the choice of σ could be:

$$\sigma(U) = 1 - \frac{1}{2}\left(\tanh\left(\frac{U - \frac{U_f + U_u}{2}}{\triangle_\sigma}\right) + 1\right), \tag{41}$$

where $U = \sqrt{u^2 + v^2} \geq 0$ is the instantaneous vessel speed, and $\triangle_\sigma > 0$ shapes the steepness of the transitional zone from full actuation to underactuation. By denoting the sway control force for a fully actuated vessel as $\tau_{2,f}$ and for an underactuated vessel as $\tau_{2,u}$ $(= 0)$, the actual sway control force enforced at any time can be represented by:

$$\tau_2 = \sigma\tau_{2,f} + (1 - \sigma)\tau_{2,u}. \tag{42}$$

Likewise, the actual sway stabilizing function can be represented by:

$$\alpha_2 = \sigma\alpha_{2,f} + (1 - \sigma)\alpha_{2,u}, \tag{43}$$

where the stabilizing function for a fully actuated vessel is given by $\alpha_{2,f} = v_d$ and for an underactuated vessel by $\alpha_{2,u}$, which is calculated from the assigned dynamics given by (36) as mentioned previously.

As defined in [10], the course angle χ is the orientation of the velocity vector of a vessel, the heading angle ψ is the orientation of the vessel itself, while the sideslip angle β is the difference between the course angle and the heading angle. The desired heading angle is thus computed by:

$$\psi_d = \chi_d - \beta, \tag{44}$$

where the desired course angle χ_d is given by (10). Higher order derivatives are generated by processing ψ_d through a reference model which is adjusted to the closed loop vessel dynamics. This expression holds unaffected of the given actuator capability of the vessel in question, and represents a guidance system with convergence to a desired geometric path as its primary task objective.

The desired surge and sway speeds are calculated by:

$$u_d = U_d \cos\beta_d \tag{45}$$

$$v_d = U_d \sin\beta_d, \tag{46}$$

where U_d is the desired linear speed of the vessel, while β_d represents the desired sideslip angle given by:

$$\beta_d = \chi_d - \psi_c, \tag{47}$$

where ψ_c is the commanded heading of a fully actuated vessel, which has the capability to control the course and heading independently. It can be given directly by a human operator or through a high-level decision making system.

To sum up, the velocity and heading controller relies upon the guidance-based path following approach to guarantee positional convergence [4], while the speed-weighted sway force (42) and stabilizing function (43) are crucial for the validity of (36) and (37), i.e. that the controller structure is equally effective for both fully actuated and underactuated marine surface vessels, seamlessly across the entire speed regime.

V. Case Study: Automatic Control Through the Key Part of the Speed Envelope

For the sake of illustration, a simulation is performed with a vessel executing a straight line maneuver while being exposed to a constant environmental force acting from the north, size 1 N. The vessel data is taken from Cybership 2, a 1:70 scale model of an offshore supply vessel, with a mass of $m = 23.8\ kg$ and a length of $L = 1.255\ m$ [5]. A full scale vessel typically becomes underactuated at speeds between $3-4\ knots$, i.e. $1.5-2\ m/s$, which corresponds to $0.2-0.27$ m/s for the model ship Cybership 2 when assuming equal Froude numbers. Hence, the transition variable σ is modelled after (41), with $U_f = 0.15$, $U_u = 0.25$ and $\triangle_\sigma = 0.05$.

The initial vessel states are chosen as $\boldsymbol{\eta}_0 = [-10\ (m), 3\ (m), 0\ (rad)]^\top$ and $\boldsymbol{\nu}_0 = [0.1\ (m/s), 0\ (m/s), 0\ (rad/s)]^\top$. The desired vessel speed U_d is equal to the initial vessel speed for the first 200 seconds, at which time it is raised to $0.3\ m/s$. Hence, the vessel is subjected to two key speeds from its speed envelope, experiencing both full actuation and underactuation during the run. The initial path parametrization variable is set to $\theta_0 = 0$, the guidance parameter $\gamma = 100$ and the lookahead distance in the guidance law is chosen to be $\triangle = 3L$. The controller gains are chosen as $k_1 = 10$ and $\mathbf{K}_2 = 10\mathbf{I}$, while $\boldsymbol{\Gamma} = \mathbf{I}$.

Figure 3 shows that the vessel heading is tangential to the path during the early part of the run, changing towards the environmental disturbance (weathervaning) as the vessel becomes underactuated due to its speed change. Figure 4 illustrates that the cross-track error converges to zero independent of the instantaneous actuator capability of the vessel.

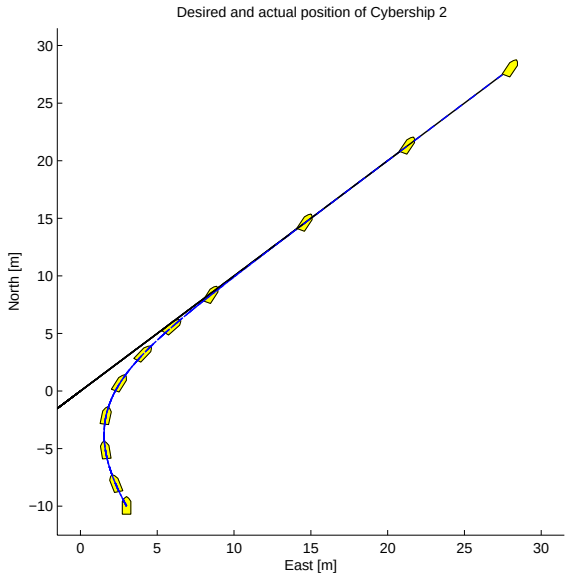

Fig. 3. Cybership 2 converges naturally to the desired geometric path.

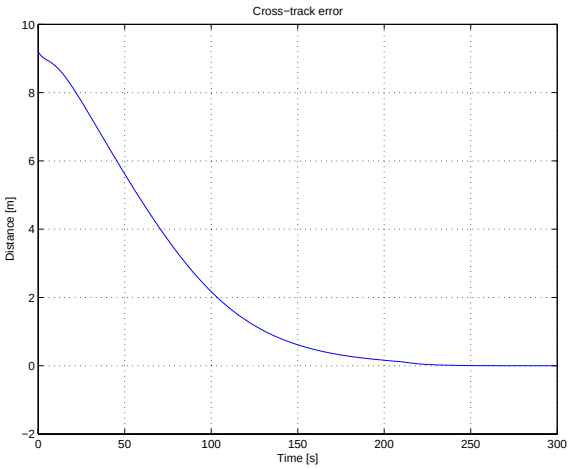

Fig. 4. The cross-track error converges to zero.

VI. Conclusions

A single controller structure has been proposed for the automatic control of a marine surface vessel through its entire speed envelope. The design is made possible by a nonlinear, model-based velocity and heading controller relying on a guidance-based path following concept necessary to ensure geometric path convergence. It guarantees that a vessel which is fully actuated at low speeds, but becomes underactuated at high speeds, is able to converge to and follow a desired geometric path independent of its speed. The result seems interesting from both a theoretical and industrial viewpoint, and the concept could contribute to reducing heuristics usually involved in industrial implementations. Simulation results successfully demonstrate the capability of the proposed guidance and control scheme.

References

[1] D. Bertin and L. Branca, "Operational and design aspects of a precision minewarfare autopilot," in *Proceedings of the Warship 2000, London, UK*, 2000.

[2] C. G. Källström, "Autopilot and track-keeping algorithms for high-speed craft," *Control Engineering Practice*, vol. 8, pp. 185–190, 2000.

[3] J. P. Strand, T. Lauvdal, and A. K. Ådnanes, "Compact azipod propulsion on DP supply vessels," in *Proceedings of the Dynamic Positioning Conference, Houston, Texas, USA*, 2001.

[4] M. Breivik and T. I. Fossen, "Path following for marine surface vessels," in *Proceedings of the OTO'04, Kobe, Japan*, 2004.

[5] R. Skjetne, "The maneuvering problem," Ph.D. dissertation, Norwegian University of Science and Technology, Trondheim, Norway, 2005.

[6] F. A. Papoulias, "Bifurcation analysis of line of sight vehicle guidance using sliding modes," *International Journal of Bifurcation and Chaos*, vol. 1, no. 4, pp. 849–865, 1991.

[7] A. Teel, E. Panteley, and A. Loría, "Integral characterization of uniform asymptotic and exponential stability with applications," *Mathematics of Control, Signals, and Systems*, vol. 15, pp. 177–201, 2002.

[8] T. I. Fossen, *Marine Control Systems: Guidance, Navigation and Control of Ships, Rigs and Underwater Vehicles*, 1st ed. Marine Cybernetics, Trondheim, Norway, 2002.

[9] T. I. Fossen, M. Breivik, and R. Skjetne, "Line-of-sight path following of underactuated marine craft," in *Proceedings of the 6th IFAC MCMC, Girona, Spain*, 2003.

[10] M. Breivik and T. I. Fossen, "Path following of straight lines and circles for marine surface vessels," in *Proceedings of the 6th IFAC CAMS, Ancona, Italy*, 2004.